Article

Vesicle Leakage Reflects the Target Selectivity of Antimicrobial Lipopeptides from *Bacillus subtilis*

Sebastian Fiedler[1,*] and Heiko Heerklotz[1,2,3,*]

[1]Leslie Dan Faculty of Pharmacy, University of Toronto, Toronto, Ontario, Canada; [2]Institute for Pharmaceutical Sciences, University of Freiburg, Freiburg, Germany; and [3]BIOSS Centre for Biological Signalling Studies, Freiburg, Germany

ABSTRACT Cyclic lipopeptides act against a variety of plant pathogens and are thus highly efficient crop-protection agents. Some pesticides contain *Bacillus subtilis* strains that produce lipopeptide families, such as surfactins (SF), iturins (IT), and fengycins (FE). The antimicrobial activity of these peptides is mainly mediated by permeabilizing cellular membranes. We used a fluorescence-lifetime based leakage assay to examine the effect of individual lipid components in model membranes on lipopeptide activity. Leakage induction by FE was strongly inhibited by cholesterol (CHOL) as well as by phosphatidylethanolamine (PE) and -glycerol (PG) lipids. Already moderate amounts of CHOL increased the tolerable FE content in membranes by an order of magnitude to 0.5 FE per PC + CHOL. This indicates reduced FE-lipid demixing and aggregation, which is known to be required for membrane permeabilization and explains the strong inhibition by CHOL. Ergosterol (ERG) had a weak antagonistic effect. This confirms results of microbiological tests and agrees with the fungicidal activity and selectivity of FE. SF is known to be much less selective in its antimicrobial action. In line with this, liposome leakage by SF was little affected by sterols and PE. Interestingly, PG increased SF activity and changed its leakage mechanism toward all-or-none, suggesting more specific, larger, and/or longer-lived defect structures. This may be because of the reduced energetic cost of locally accumulating anionic SF in an anionic lipid matrix. IT was found largely inactive in our assays. *B. subtilis* QST713 produces the lipopeptides in a ratio of 6 mol SF: 37 mol FE: 57 mol IT. Leakage induced by this native mixture was inhibited by CHOL and PE, but unaffected by ERG and by PG in the absence of PE. Note that fungi contain anionic lipids, but little PE. Hence, our data explain the strong, fungicidal activity and selectivity of *B. subtilis* QST713 lipopeptides.

INTRODUCTION

Microorganisms that exhibit antagonistic activities against plant pathogens are widely used as environmentally friendly crop-protection agents (1). A product used in the field, under the name Serenade, utilizes the *Bacillus subtilis* strain QST713. This particular strain produces a mixture of three different lipopeptide families, namely surfactins, iturins, and fengycins, which act against at least 10 fungal, 4 oomycetal, and 2 bacterial phytopathogens. Isolated from the native mixture, both iturins (2) and fengycins (3) exhibit mainly antifungal activity, whereas surfactins display a broad range of antimicrobial actions including antibacterial (4) and antiviral (5,6) activities. In addition, surfactins and iturins possess a pronounced hemolytic activity, whereas fengycins exhibit low levels of hemolysis (1). A large body of evidence suggests that the antimicrobial activity of these lipopeptides relies on their permeabilization of the target-cell membrane (1).

All three peptide families exhibit an overall amphiphilic character, possess surface activity (7), and interact readily with lipid membranes (8-10), which directly relates to their ability to permeabilize membranes. The structures of surfactins and iturins consist of cyclic heptapeptides linked to β-hydroxy fatty acid chains (C_{13}–C_{15}) and β-amino fatty acid chains (C_{14}–C_{17}), respectively (Fig. S1 in the Supporting Material) (1). Fengycins represent cyclic decapeptides connected to β-hydroxy fatty acid chains (C_{14}–C_{18}) (1).

The lipid composition of monolayers and bilayers has been shown to affect, for example, penetration depth, membrane partitioning, or leakage potency of lipopeptides. Most data exist on surfactins, for which the penetration depth in lipid monolayers varies with the lipid headgroup in the order of 1,2-dimyristoyl-*sn*-glycero-3-phosphatidylcholine (DMPC) > 1,2-dimyristoyl-*sn*-glycero-3-phosphatidylethanolamine (DMPE) ≫ 1,2-dimyristoyl-*sn*-glycero-3-phosphatidic acid (DMPA) (11). Moreover, PE reduces membrane leakage by surfactins (12). In addition, surfactins interact with negatively charged lipids and, for example, transform giant unilamellar vesicles (GUVs) composed of 1-palmitoyl-2-oleoyl-*sn*-glycero-3-phosphatidylglycerol (POPG) into small unilamellar vesicles (13). Cholesterol (CHOL) was reported to attenuate the membrane-perturbing effect of surfactins (12,14), irrespective of an unaltered penetration depth measured in egg lecithin monolayers containing 30 mol% CHOL (11).

Mycosubtilin, one of the best-studied peptides of the iturin family, forms clusters in DMPC monolayers (15)

Submitted July 9, 2015, and accepted for publication September 21, 2015.

*Correspondence: mail@sebastianfiedler.net or heiko.heerklotz@pharmazie.uni-freiburg.de

Editor: Klaus Gawrisch

0006-3495/15/11/2079/11

http://dx.doi.org/10.1016/j.bpj.2015.09.021

and specifically interacts with CHOL and ergosterol (ERG) (16). Notably, iturin A did not induce carboxyfluorescein (CF) leakage in large unilamellar vesicles of various lipid compositions (17). This proved to be true for our experiments, too. Iturins did not show leakage in any of the tested lipid compositions (data not shown). This inactivity in vesicle leakage assays is most likely a consequence of methodological limitations, because iturin A induces CF leakage in erythrocyte ghosts, for example (17).

Fengycins form clusters in membranes composed of 1,2-dipalmitoyl-*sn*-glycero-3-phosphatidylcholine (DPPC) (18,19). The lipopeptide does not mix well with 1-palmitoyl-2-oleoyl-*sn*-glycero-3-phosphatidylcholine (POPC) membranes and induces all-or-none leakage at very low concentrations in the membrane (10). In a coarse-grained molecular dynamic (MD) simulation (20), fengycin clusters caused stronger membrane perturbations than monomers. Furthermore, the same MD simulation found that a positively charged ornithine side chain of fengycin attracts negatively charged POPG headgroups thereby competing with cluster formation of lipopeptides. In combined atomic force microscopy and Langmuir trough studies (21), fengycins preferentially partition into CHOL-rich membranes and directly interact with CHOL. Despite these detailed studies on specific lipopeptide-lipid systems, how these molecular interactions relate to antimicrobial activity warrants further investigation.

More recently, Avis and co-workers (22) reported that minimum inhibitory concentrations (MICs) of fengycin A against four fungal pathogens correlate with certain features of fungal cellular membranes. The data suggest that fengycin A is most active against fungal membranes with low contents of ERG, low fractions of anionic lipids, and high fractions of PE. Such correlations of lipopeptide MICs and fungal membrane features imply that lipid composition may be a major determinant for target-cell selection of fengycins and presumably also of other *B. subtilis* lipopeptides. In biological membranes, however, all these (and many more) parameters vary in parallel from one species to another. The identification of correlations that indeed represent causal relationships would require a systematic analysis under easier to control conditions. In vitro model membranes represent such a complementary approach allowing for precise control of the membrane composition and variation of individual components. Thus, in such simpler, well-defined in vitro systems, it is more likely that we isolate membrane properties that unequivocally alter lipopeptide activities. Conversely, the relevance of our studies on model membranes needs to be verified in more complex biological systems, as done by Avis and co-workers (22). In consequence, the combination of model-membrane data and cellular data can yield general features that relate to the sensitivity of cellular membranes to *B. subtilis* lipopeptides.

The intention of our study is to test the leakage propensity of *B. subtilis* lipopeptides in model membranes that represent or oppose the key features of their potential target membranes. One key feature that distinguishes fungal membranes from those of other organisms is the presence of ERG as the main sterol component (23). CHOL represents the typical sterol of mammalian cell membranes (23), whereas bacteria in general lack sterols in their membranes. Thus, we first checked if sterols serve as a marker for antifungal activity of *B. subtilis* lipopeptides by comparing leakage in POPC vesicles containing various amounts of either ERG or CHOL. Second, we investigated the effect of negatively charged membranes because fungal cellular membranes generally display less negative surface charge than bacterial cellular membranes (24,25). Third, we analyzed the impact of negative curvature strain facilitated by incorporation of PE into PC membranes; and fourth, we tested the effect of a mixed PG/PE membrane more representative of bacteria (26).

MATERIALS AND METHODS

Materials

Calcein, cholesterol, ergosterol, ethylenediaminetetraacetic acid (EDTA) NaCl, and tris(hydroxymethyl)aminomethane (TRIS) were purchased from Sigma-Aldrich (Oakville, Ontario, Canada) at highest purity available. 1-palmitoyl-2-oleoyl-*sn*-glycero-3-phosphatidylcholine (POPC), 1-palmitoyl-2-oleoyl-*sn*-glycero-3-phosphatidylethanolamine (POPE), and 1-palmitoyl-2-oleoyl-*sn*-glycero-3-phosphatidylglycerol (POPG) were purchased as chloroform stocks from Avanti Polar Lipids (Alabaster, AL). Four different solutions containing cyclic lipopeptides extracted from *Bacillus subtilis* strain QST713 were provided by Bayer CropScience (Davis, CA): 1) a natural extract containing surfactins, iturins, and fengycins (SF/IT/FE mix) in a molar ratio of 6:57:37; 2) a mixture of surfactins of the sequence Glu/Gln-Val/Leu/Ile-Leu-Ala/Val/Leu/Ile-Asp-Leu-Val/Leu/Ile (surfactins carry β-hydroxy-fatty acids of 13 to 15 carbon atoms, form micelles in aqueous solution (CMC $\approx$ 7.5 μM), have an average molecular weight of 1036 g/mol, and are negatively charged at pH 8.5 and 110 mM NaCl); 3) a mixture of iturins of the sequence Asn-Tyr-Asn-Pro/Gln/Ser-Pro/Gln/Glu-Ser/Asn-Thr/Ser/Asn (iturins carry β-amino-fatty acids of 14 to 17 carbon atoms, form micelles in aqueous solution, and have an average molecular weight of 1060 g/mol); 4) a mixture of fengycins of the sequence Glu-Orn-Tyr-Thr-Glu-Ala/Val-Pro-Gln/Glu-Tyr-Ile (fengycins carry β-hydroxy-fatty acids of 14 to 18 carbon atoms, form micelles in aqueous solution, have an average molecular weight of 1450 g/mol, and are negatively charged at pH 8.5 and 110 mM NaCl (10)).

Preparation of calcein-loaded vesicles

Lipid vesicles were prepared according to standard procedures (27). In brief, phospholipid dissolved in chloroform was transferred gravimetrically into glass vials and dried for 6 h. For phospholipid-phospholipid and/or phospholipid-sterol mixtures, phospholipid or sterol in chloroform was added gravimetrically to the dry phospholipid film to yield appropriate molar ratios, vortexed, and dried again for 6 h. Lipid films were hydrated in buffer A (70 mM calcein, 10 mM TRIS pH 8.5, 0.5 mM EDTA, 110 mM NaCl) and subjected to 10 freeze-thaw cycles followed by 15 cycles of extrusion using polycarbonate track-etched membranes of 100 nm pore size (GE, Mississauga, Canada) in a LIPEX 10-mL thermobarrel extruder by Northern Lipids (Burnaby, Canada). Hydrodynamic diameters of vesicles were monitored by dynamic light scattering using a Zetasizer Nano ZS by Malvern Instruments (Malvern, UK). Vesicles were loaded

on PD-10 gel filtration columns (GE) equilibrated with buffer B (10 mM TRIS pH 8.5, 0.5 mM EDTA, and 110 mM NaCl) to yield entrapped-to-free ratios of calcein ≥ 10. Phospholipid concentration was determined by a colorimetric phosphate assay (BioVision, Milpitas, CA).

Time-resolved fluorescence acquisition

Fluorescence decays were acquired on a Fluorolog 3 time-resolved single photon counting instrument from Horiba (Edison, NJ) at a temperature of 20°C. For excitation, a laser diode was used, emitting at a wavelength of 467 nm and at a pulse rate of 1 MHz. Count frequency was kept <20 kHz by the use of gray filters. Fluorescence emission was guided through a double-grated monochromator at $\lambda = 515$ nm and a band width of 2 nm, and a TBX detector (Horiba) was used for data recording. Signal was accumulated for 180 s to yield ~10^4 peak counts. Data were analyzed by the software DAS6 (Horiba). The following biexponential decays were convoluted with the instrument response function and fitted to the experimental data:

$$I(t) = A + B_E e^{-t/\tau_E} + B_F e^{-t/\tau_F}, \quad (1)$$

where A represents baseline counts; B_E and B_F are the preexponential factors of the individual lifetimes, τ_E and τ_F, respectively, and t stands for the time.

Lifetime-based leakage assay

To assess membrane permeabilization, we exploited the concentration dependence of the fluorescence lifetime of calcein (10,28-30). In brief, calcein was loaded into vesicles at a high concentration of ~70 mM, which leads to collisional self-quenching and short fluorescence lifetime of the entrapped dye, τ_E (0.3 to 0.4 ns). Unquenched calcein in dilute solution displays a fluorescence lifetime, τ_F, which is roughly 10 times longer (~4 ns) than τ_E. Release from vesicles dilutes calcein, reduces self-quenching, and alters the relative fractions of signal contributions with τ_E and τ_F. The preexponential factors B_E and B_F (Eq. 1), the (weak) contribution of free dye in the absence of permeabilizer, B_{F0}, and a static quenching factor, Q_{stat}, yield the dye efflux, E, as in the following:

$$E = (B_F - B_{F0})/(B_F - B_{F0} + Q_{stat}B_E), \quad (2)$$

which directly correlates with membrane permeabilization. In addition, the assay distinguishes between graded leakage (small/transient pores) and all-or-none leakage (large/stable pores) (31). In graded leakage, a fraction of calcein remains inside leaky vesicles; this partial dilution of entrapped dye corresponds to an intermediate value of τ_E. In all-or-none leakage, τ_E remains constant, because samples include only entirely intact vesicles and entirely leaked vesicles.

A theoretical lifetime of entrapped dye in the case of ideal homogenously graded leakage, τ_{EI}, can be calculated using the following equation:

$$\tau_{EI} = \tau_0/(1 + K\, c_{DE}), \quad (3)$$

where τ_0 is the lifetime of the dye in the absence of quenching, K is the Stern-Volmer constant, and c_{DE} is the concentration of entrapped dye. The following equation:

$$K = (\tau_{E0} - 1)/c_{DE0}, \quad (4)$$

yields K with τ_{E0} and c_{DE0} being the lifetime and the concentration of the entrapped dye in the absence of membrane perturbants, respectively.

In a leakage experiment, lipopeptides were diluted into buffer B to yield a final volume of 1990 μL, to which 10 μL of calcein loaded vesicles were added at a final phospholipid concentration of 30 μM. Samples were incubated on a rotatory shaker for 1 h, and then fluorescence decays were recorded. Phospholipid concentrations of 100, 200, and 300 μM were incubated at lower volumes (<500 μL). Before data acquisition, the volume was adjusted to 2 mL.

RESULTS

Leakage of POPC vesicles

We first performed leakage experiments in pure POPC vesicles, which served as a reference to assess how different types of membrane compositions affect membrane leakage by *B. subtilis* QST713 lipopeptides. To this end, we utilized either SF/IT/FE mix (natural lipopeptide extract from *B. subtilis* QST713) or the isolated fractions of fengycins and surfactins as membrane perturbants. As mentioned in the Introduction, iturins did not induce leakage in any of the tested model membranes (data not shown).

The SF/IT/FE mix released most of the dye from POPC vesicles within a concentration range of 5 to 10 μM (*open squares* in Fig. 1 *A*). To assess the leakage mechanism (28,31), we routinely plotted τ_E against the lipopeptide concentration and compared this with the curve of τ_{EI}, as calculated assuming ideal, homogeneously graded leakage using Eq. 3. Such a plot is, for example, Fig. 1 *D*, but the results for leakage of pure POPC by SF/IT/FE mix are shown in Fig. S2 *B*. The data there show that τ_E stays largely constant also at values of E, at which graded leakage should cause a

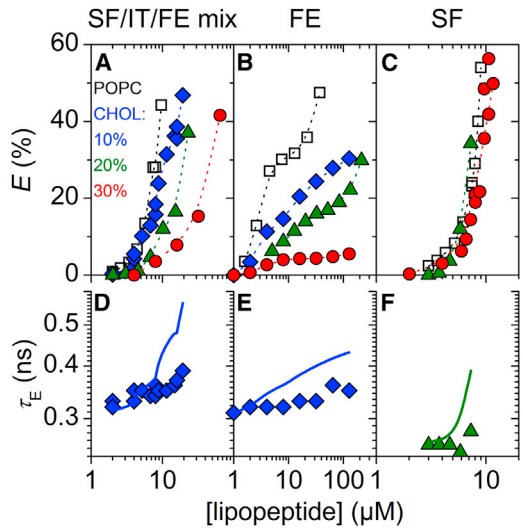

FIGURE 1 Leakage of vesicles composed of 30 μM POPC-containing cholesterol (CHOL) induced by surfactins (SF)/iturins (IT)/fengycins (FE) natural mixture (*left*: *A*/*D*), FE (*center*: *B*/*E*), and SF (*right*: *C*/*F*), respectively. (*A–C*) Dye efflux after 1 h, E, as a function of lipopeptide concentration. Dotted lines are to guide the eye only. (*D–F*) Lifetime of entrapped dye, τ_E, as a function of lipopeptide concentration. Solid lines simulate τ_E for ideal homogeneously graded leakage (Eqs. 3 and 4). For clarity, only τ_E values of 10 or 20 mol% CHOL are shown. Refer to Fig. S5 for τ_E at other sterol contents. Squares, diamonds, triangles, and circles represent pure POPC, 10, 20, and 30 mol% CHOL, respectively. To see this figure in color, go online.

significant increase, implying that SF/IT/FE mix displayed all-or-none leakage of POPC vesicles. Fengycin-induced leakage of pure POPC vesicles displayed a steep increase in E within a concentration range of 1 to 5 μM (Fig. 1 *B*). At concentrations >5 μM, E leveled off at ~30%, and only concentrations >20 μM led to values of $E > 30\%$. The plateau region of the fengycin leakage curve has previously been attributed to a low membrane solubility and crystal formation (10). Fengycins permeabilized POPC vesicles following an all-or-none mechanism (Fig. 3 *C*), which is in agreement with previous experiments (10). Surfactins exhibited a steep increase in E within a concentration range of 1 to 10 μM and caused graded leakage (Figs. 1 *C* and 3 *D*), as reported previously (32).

Antifungal lipopeptides are more inhibited by cholesterol than by ergosterol

Next, we assessed lipopeptide-induced leakage of POPC vesicles supplemented with 10 to 30 mol% CHOL (Fig. S3) and ERG (Fig. S4), respectively (Fig. 1). To compare leakage efficiencies at different lipid compositions, we employed lipopeptide concentrations required to reach $E = 20\%$, $c^{\mathrm{LP}}_{\mathrm{E20}}$, as summarized in Table 1.

In comparison with pure POPC, CHOL inhibited vesicle leakage by SF/IT/FE mix (Fig. 1 *A*), as indicated by increased values of $c^{\mathrm{SF/IT/FE}}_{\mathrm{E20}}$ (Table 1). A bilayer content of 10 mol% CHOL showed a modest inhibition and the leakage curve fell closely to the one obtained in the absence of CHOL. However, the inhibitory effect was much more pronounced at 20 and 30 mol% CHOL. ERG at 10 mol% caused modest inhibition (Fig. 2 *A*), reaching similar levels of E as 10 mol% CHOL. Interestingly, inhibition of SF/IT/FE-mix leakage by 30 mol% ERG was much weaker than inhibition by 30 mol% CHOL and rather comparable with the effect of 10 mol% ERG. Despite the attenuating effects shown by both sterols, the leakage mechanism of SF/IT/FE mix in POPC/CHOL and POPC/ERG remained all-or-none, as in POPC (Figs. 1 *D*, 2 *D*, and S2 *B*).

Both CHOL and ERG inhibited leakage by fengycins (Figs. 1 *B* and 2 *B*; also refer to Discussion). In particular, CHOL contents of 10 and 20 mol% exerted substantial inhibitory effects, and 30 mol% of CHOL essentially inactivated fengycins. The attenuating effect caused by 10 mol% ERG was comparable with the impact of 10 mol% CHOL. Similar to SF/IT/FE mix, 30 mol% ERG were less efficient in fengycin inhibition than 30 mol% CHOL. The leakage mechanism of fengycins remained all-or-none irrespective of the presence of sterols (Figs. 1 *E*, 2 *E*, and 3 *E*).

Sterols do not change extent, but mechanism of surfactin-induced leakage

Both CHOL and ERG had little effect on the leakage potency of surfactins (Figs. 1 *C* and 2 *C*). Despite this limited impact on leakage, both sterols changed leakage from homogeneously graded in pure POPC vesicles (Fig. 3 *D*) toward more heterogeneous leakage mechanisms (Figs. 1 *F* and 2 *F*). This is exemplified by the systematic difference among τ_{E} values obtained in the absence and presence of 20 mol% CHOL at different POPC concentrations (Fig. 3, *D* and *F*). In the absence of CHOL, values of τ_{E} at $E > 20\%$ agreed well with simulated graded leakage, whereas in the presence of CHOL they deviated substantially from the model. We did not observe notable differences in terms of the leakage mechanism between the two sterols.

Cholesterol increases the tolerable fraction of fengycins in POPC membranes

There are two possible explanations for the inhibition of the lipopeptides by CHOL. It may 1) hinder the lipopeptides from partitioning into the membrane in the first place, or 2) enable the membrane to accommodate higher lipopeptide contents without being disrupted. To distinguish the two, we determined the lipopeptide-to-phospholipid ratio in the membrane, R_{e}, of fengycins causing 10% efflux in the presence and absence of 20 mol% CHOL (Figs. 3 *A* and 4). Briefly, leakage curves acquired at various lipid concentrations (Fig. 3 *A*) serve to obtain equi-activity plots (28,33) (Fig. 4), in which lipopeptide concentrations for a particular value of E are plotted against the corresponding lipid concentrations (28). Linear fits to equi-activity data by the equation

$$c_{\mathrm{P}} = R_{\mathrm{e}} c_{\mathrm{POPC}} + c^{\mathrm{aq}}_{\mathrm{P}} \qquad (5)$$

yield R_{e} and the aqueous lipopeptide concentration, $c^{\mathrm{aq}}_{\mathrm{P}}$.

Equi-activity plots for $E = 10\%$ of both pure POPC and POPC/20% CHOL were linear and fitted in terms of Eq. 5

TABLE 1 Summary of $c^{\mathrm{LP}}_{\mathrm{E20}}$ values obtained for lipopeptide-induced leakage of model membranes

	POPC								POPG	POPE
	(mol%)	CHOL (mol%)			ERG (mol%)		POPE (mol%)		(mol%)	POPG (mol%)
	100	10	20	30	10	30	20	40	100	40
$c^{\mathrm{SF/IT/FE\ mix}}_{\mathrm{E20}}$ (μM)	6.5	8.5	16	35	8	10	26.4	>20	6.8	>95
$c^{\mathrm{FE}}_{\mathrm{E20}}$ (μM)	3.3	16	110	>128	16	49	60	>42	105	>105
$c^{\mathrm{SF}}_{\mathrm{E20}}$ (μM)	7	n.d.	6.4	7.8	6	5.1	9.8	13.5	3.5	90

$c^{\mathrm{LP}}_{\mathrm{E20}}$ is the molar concentration needed to induce 20% calcein efflux from 30 μM phospholipid vesicles after 1 h incubation.

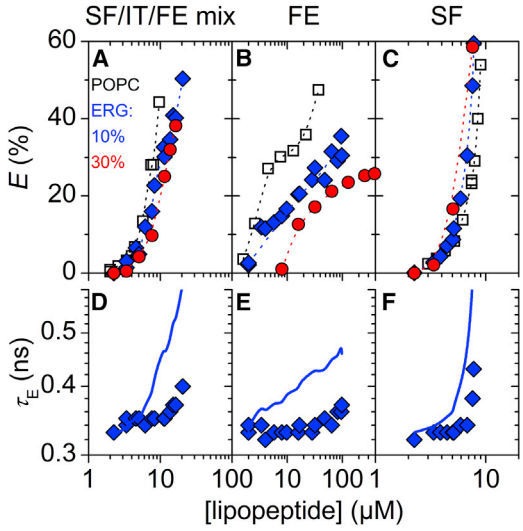

FIGURE 2 Leakage of vesicles composed of 30 μM POPC-containing ergosterol (ERG) induced by surfactins (SF)/iturins (IT)/fengycins (FE) natural mixture (*left*: *A*/*D*), FE (*center*: *B*/*E*), and SF (*right*: *C*/*F*), respectively. (*A–C*) Dye efflux after 1 h, *E*, as a function of lipopeptide concentration. Dotted lines are to guide the eye only. (*D–F*) Lifetime of entrapped dye, τ_E, as a function of lipopeptide concentration. Solid lines simulate τ_E for ideal homogeneously graded leakage (Eqs. 3 and 4). For clarity, only τ_E values of 10 mol% ERG are shown. Refer to Fig. S5 for τ_E at other sterol contents. Squares, diamonds, triangles, and circles represent pure POPC, 10, 20, and 30 mol% ERG, respectively. To see this figure in color, go online.

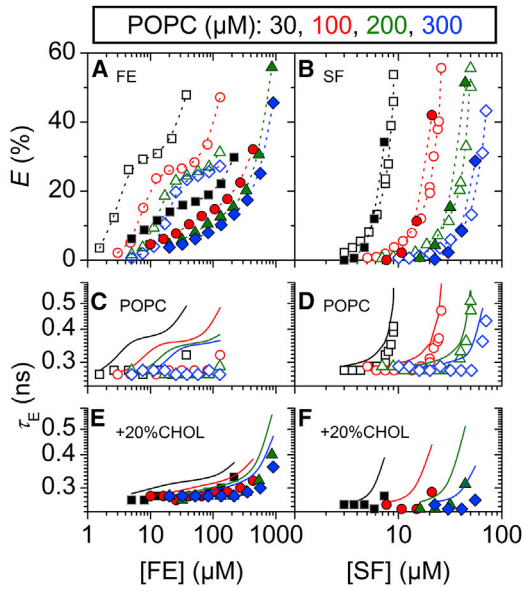

FIGURE 3 Effect of cholesterol on vesicle leakage induced by fengycins (FE; *left*) and surfactins (SF; *right*) at various lipid concentrations. (*A* and *B*) Efflux, *E*, from vesicles of POPC (*open*) and POPC/20 mol% CHOL (*solid*), respectively, after 1 h as a function of FE (*A*) and SF (*B*) concentrations. Squares, circles, triangles, and diamonds indicate POPC concentrations of 30, 100, 200, and 300 μM, respectively. Dotted lines are to guide the eye only. (*C–F*) Lifetime of entrapped dye, τ_E, as a function of FE (*C* and *E*) and SF (*D* and *F*) concentrations. Solid lines simulate τ_E for ideal homogeneously graded leakage (Eqs. 3 and 4). To see this figure in color, go online.

(Fig. 4). The values of R_e and c_P^{aq} of fengycins to induce $E =$ 10% obtained in the absence of CHOL (Table 2), and their corresponding *K*, agree with those published previously (10). In the presence of CHOL, about an eightfold higher membrane content, R_e, of fengycins is required to induce the same degree of leakage compared with the CHOL-free membrane. That suggests that POPC/20% CHOL vesicles can incorporate rather large amounts of fengycins without becoming permeabilized.

It has been explained (33) that equi-activity plots typically yield R_e with very good precision. By contrast, errors of c_P^{aq} can become prohibitively large for compounds with strong membrane partitioning, for which the intercept becomes indistinguishable from zero. In our study, this was the case for fengycin interacting with CHOL-containing membranes. For the other samples, the apparent partition coefficients, K_R, were derived as

$$K_R \equiv \frac{R_e}{c_P^{aq}} \tag{6}$$

and listed in Table 2. Recall that we had defined R_e to refer to POPC only (Fig. 4), so that the same applies to K_R (Eq. 6). The so-defined partition coefficient of detergents was reported to be largely conserved upon addition of CHOL (34), in line with our finding for surfactin (Table 2). Note that a partition coefficient referring to all lipid (POPC + CHOL) would be lower by a factor of 0.8 at 20 mol% CHOL.

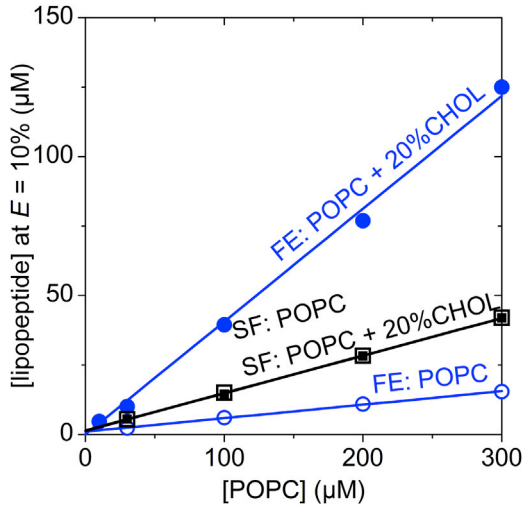

FIGURE 4 Equi-activity plot of fengycin-induced leakage in vesicles of POPC (*open*) and of POPC/20% CHOL (*solid*). Fengycin (*blue circles*) and surfactin (*black squares*) concentrations required to cause efflux, *E*, of 10% as a function of the POPC concentration. Lines are linear fits using Eq. 5. Note that for surfactins open and solid squares coincide. Refer to Fig. 3 for corresponding leakage experiments. To see this figure in color, go online.

TABLE 2 Cholesterol dependence of fengycin and surfactin partitioning into POPC vesicles (Eqs. 5 and 6) at $E = 10\%$

Fengycins	R_e ($E = 10\%$)	c_P^{aq} (μM)	K_R (mM^{-1})
POPC	0.05	1.06	46
POPC/CHOL 20 mol%	0.41	–	–
Surfactins			
POPC	0.13	1.46	92
POPC/CHOL 20 mol%	0.14	1.31	103

R_e, lipopeptide-to-lipid ratio in the membrane; c_P^{aq}, aqueous concentration of lipopeptides; K_R, apparent partition coefficient. Note that R_E and K_R refer to the POPC component only; they would decrease by a factor of 0.8 if CHOL is included in the nominal lipid concentration. For fengycins in POPC/CHOL 20%, the value obtained for c_P^{aq} was much smaller than the associated error.

Cholesterol does not affect membrane partitioning of surfactins

The leakage potency of surfactins was largely unaffected by the presence of CHOL at a POPC concentration of 30 μM. We confirmed this finding by obtaining additional leakage data at POPC concentrations of 100, 200, and 300 μM in the presence and absence of 20 mol% CHOL (Fig. 3 *B*). Though leakage shifted to higher surfactin concentrations at higher lipid concentrations, there was no substantial difference between E values of pure POPC and of POPC/20%CHOL at identical phospholipid concentrations. Accordingly, equi-activity data obtained at $E = 10\%$ of both POPC and POPC/20% CHOL coincide (Fig. 4) and membrane partitioning parameters showed only minor changes (Table 2).

Negative surface charge of membranes inhibits fengycins but activates surfactins

We assessed how negatively charged lipids affect the ability of *B. subtilis* lipopeptides to permeabilize membranes, because many bacteria display negatively charged membrane surfaces. For this purpose, we determined leakage efficiencies of SF/IT/FE mix, fengycins, and surfactins in vesicles composed of POPG. A summary on the impact of negative surface charge based on c_{E20}^{LP} can be found in Table 1.

Leakage by SF/IT/FE mix was unaffected by POPG, as indicated by the superimposing leakage curves obtained for POPG and POPC (Fig. 5 *A*). The leakage mechanism of SF/IT/FE mix in POPG (Fig. 5 *D*) is somewhat different from the clear-cut all-or-none seen for POPC (Fig. S2 *B*). It appears that also vesicles developing no efflux-all pore show some partial dye release (all-or-some).

Fengycins caused much less leakage in POPG vesicles than in POPC vesicles (Fig. 5 *B*). Compared with POPC, c_{E20}^{FE} in POPG increased by a factor of ~30 (Table 1). Despite this quite dramatic inhibition, the leakage mechanism resembled still an all-or-none scenario, as in POPC (Figs. 3 *C* and 5 *E*).

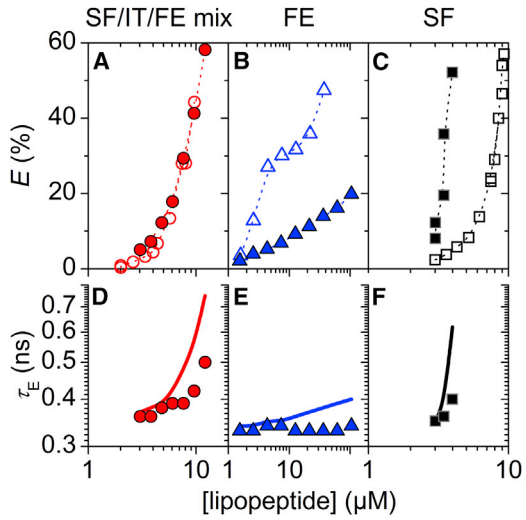

FIGURE 5 Leakage of vesicles composed of 30 μM POPG (*solid*) and 30 μM POPC (*open*) by surfactins (SF)/iturins (IT)/fengycins (FE) natural mixture (*red circles*), FE (*blue triangles*), and SF (*black squares*). (*A–C*) Dye efflux after 1 h, E, as a function of lipopeptide concentration. Dotted lines are to guide the eye only. (*D–F*) Lifetime of entrapped dye, τ_E, as a function of lipopeptide concentration. Solid lines simulate τ_E for ideal homogeneously graded leakage (Eqs. 3 and 4). To see this figure in color, go online.

Unlike fengycins, surfactins permeabilized POPG more effectively than POPC and leakage shifted to lower concentrations (Fig. 5 *C*). Similar to the result for SF/FE/IT, leakage was much less homogeneous (graded) compared with that of POPC, with some vesicles obviously losing all their dye (Figs. 3 *D* and 5 *F*).

Negative curvature strain in membranes inhibits *B. subtilis* lipopeptides

We investigated the effect of negative curvature strain by adding lipopeptides to mixed vesicles composed of POPC and POPE in molar ratios of 4:1 and 3:2, respectively. Lipopeptides are more likely to encounter PE in bacterial membranes, as fungi and mammalian cells keep this lipid mostly in their inner leaflets (25). POPE displays an overall conical shape, which induces negative curvature strain in lipid bilayers (23). Again, we utilize pure POPC as a reference to assess the effect of POPE on leakage efficiencies of *B. subtilis* lipopeptides, as summarized in Table 1.

Leakage by SF/IT/FE mix was considerably inhibited by POPE (Fig. 6 *A*). At 20 mol% POPE (POPC:POPE = 4:1), $c_{E20}^{SF/IT/FE}$ increased by a factor of 3.7, as compared with pure POPC. A further increase of the POPE content to 40 mol% (POPC:POPE = 3:2) largely abolished leakage by SF/IT/FE mix and E remained <5%.

Fengycins displayed the strongest sensitivity to POPE (Fig. 6 *B*). A POPE content of 20 mol% increased c_{E20}^{FE} by a factor of 17, and 40 mol% eliminated leakage by

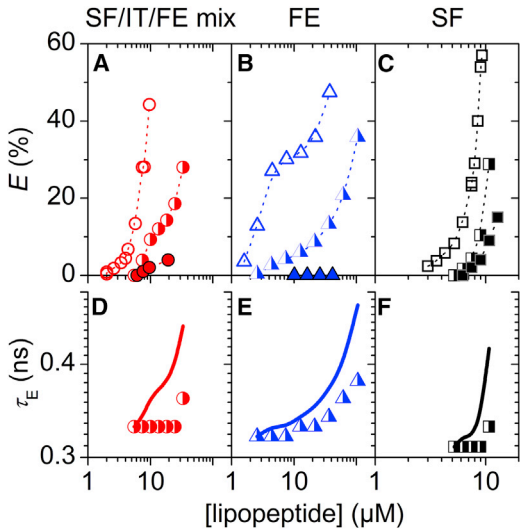

FIGURE 6 Leakage of vesicles composed of 30 μM POPC (*open*) and 30 μM POPC/POPE at molar ratios of 4:1 (*half open*) and 3:2 (*solid*), respectively. Red circles represent surfactins (SF)/iturins (IT)/fengycins (FE) natural mixture, blue triangles represent FE, and black squares represent SF. (*A–C*) Dye efflux after 1 h, *E*, as a function of lipopeptide concentration. Dotted lines are to guide the eye only. (*D–F*) Lifetime of entrapped dye, τ_E, as a function of lipopeptide concentration. Solid lines simulate τ_E for ideal homogeneously graded leakage (Eqs. 3 and 4). To see this figure in color, go online.

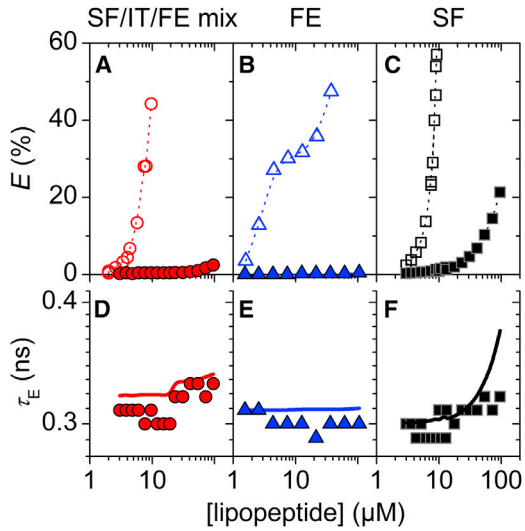

FIGURE 7 Leakage of vesicles composed of 30 μM POPC (*open*) and 30 μM POPE/POPG at a molar ratio of 3:2 (*solid*). Red circles represent surfactins (SF)/iturins (IT)/fengycins (FE) natural mixture, blue triangles represent FE, and black squares represent SF. (*A–C*) Dye efflux after 1 h, *E*, as a function of lipopeptide concentration. Dotted lines are to guide the eye only. (*D–F*) Lifetime of entrapped dye, τ_E, as a function of lipopeptide concentration. Solid lines simulate τ_E for ideal homogeneously graded leakage (Eqs. 3 and 4). To see this figure in color, go online.

fengycins. The leakage mechanism of fengycins was slightly affected by the presence of POPE, trending to a more heterogeneous mechanism at concentrations $\geq$ 36 μM (Fig. 6 *E*).

Surfactin leakage was also inhibited by PE, as reported previously (12), but the effect was much more modest than in the case of SF/IT/FE mix and fengycins (Fig. 6 *C*). The leakage mechanism switched to more heterogeneous behavior, as indicated by rather constant values of τ_E (Fig. 6 *F*).

B. subtilis lipopeptides exhibit low activity against a model for bacterial membranes

After examining the individual effects of POPG and POPE, we assessed the combined effect of these two types of lipids. This is of particular interest because PE and PG are typical lipids of bacterial cell membranes, against which SF/IT/FE mix and fengycins exhibit low activity.

Taken together, membranes composed of POPE and POPG at a molar ratio of 3:2 greatly inhibited leakage by *B. subtilis* lipopeptides (Fig. 7, *A–C*). The only lipopeptide family that induced leakage were surfactins. However, the activity was greatly diminished, and c_{E20}^{SF} increased by a factor of 13, as compared with POPC vesicles. The leakage mechanism of surfactins in POPE/POPG vesicles followed an all-or-none behavior (Fig. 7 *F*).

DISCUSSION

Fengycin leakage of model membranes matches antifungal minimum inhibitory concentration profiles

The activities of fengycins from *B. subtilis* QST713 against various model membranes fall largely in line with activities of fengycin A (*B. subtilis* CU12) against various fungal pathogens, as reported by Avis and co-workers (22). Formally, the cellular data suggest that higher antimicrobial activities of fengycin A (i.e., lower MICs) correlate with lower ERG contents, lower PG (vs. PC) contents, and higher PE contents of fungal membranes.

Our leakage data confirm the first two effects and assign the opposite effect to PE, i.e., POPE strongly inhibits leakage by fengycins (Table 1). It should be noted that the negative correlation of PE and MICs of fengycin A was also treated with caution by Avis and co-workers (22) and apparently represents a noncausal relationship. Both our leakage data as well as the cellular data (22) demonstrate that the activity of fengycins decreases with increasing ERG content of membranes. This indicates that ERG does not necessarily enhance the activity of antifungal agents, unlike in the case of Amphotericin B (35), for example. The general consensus between our fengycin leakage results and data reflecting their actual fungicidal activity (22) strengthens the idea that the composition of cellular membranes governs the activity of fengycins. Moreover, it establishes a link between membrane permeabilization and

antimicrobial activities of lipopeptides. We stress that a combination of microbiological studies and experiments with simple model systems provides superior insight.

Implications for target cell selectivity

The leakage activity displayed by fungicidal SF/IT/FE mix and fengycins in model membranes matches very well with the typical properties of fungal membranes. Most importantly, both lipopeptides caused substantially higher levels of leakage in membranes containing the fungal sterol ERG than in membranes containing the mammalian sterol CHOL (also refer to next section). Furthermore, a bacterial model membrane composed of POPE and POPG strongly reduced their leakage activities. Notably, negative membrane surface charge alone was not sufficient to inhibit leakage by SF/IT/FE mix because the strong inhibition experienced by fengycins appeared to be at least partially compensated by activation of surfactins. In fact, electrostatics is not a good selectivity criterion for agents produced by bacteria to fight other bacteria or fungi. This is by contrast to antimicrobial peptides produced by higher organisms, which often act against anionic membranes exclusively (36).

Fengycin-lipid miscibility governs enhanced selectivity

Sterol content, charge, and negative-curvature lipids are considered to govern the partitioning of antibiotic peptides into a target membrane and its membrane-destabilizing activity (37). These properties constitute unspecific criteria for a compound to act against bacteria, fungi, or mammalian cells. In our study, these default effects are exemplified rather well by surfactins (see below). Other drugs or toxins bind specifically to a certain protein or lipid in the membrane to be internalized and activated (38). Fengycins seem to utilize an intermediate mode of target selectivity. Although relatively specific interactions with membrane components govern the miscibility of fengycins within the membrane, cluster formation (18-20) activates strong, local, yet unspecific membrane destabilization. This mechanism provides an explanation for the surprising finding that CHOL-containing membranes can accommodate fengycin contents as high as ~29 mol% (R_e = 0.41 at E = 10%; Table 2) without being disrupted. One possible explanation is that CHOL may form hydrogen bonds to fengycins (21,39), which competes with fengycin aggregation and consequently reduces its membrane permeabilizing activity.

We also suggest that the lower inhibition of fengycin-induced leakage by ERG (Fig. 2 *B*), as compared with CHOL (Fig. 1 *B*), mainly relates to its lower ability to engage in specific sterol-lipopeptide interactions. In comparison with CHOL, ERG contains additional double bonds in the second ring of the steroid nucleus as well as between C22 and C23 of the alkyl side chain. In addition, the alkyl side chain features a methyl group at C24 that is absent in CHOL (Fig. S4). These structural differences render ERG more rigid than CHOL and result in a kinked conformation of its alkyl side chain (40). We speculate that these structural features of ERG (41,42) interfere with optimal hydrogen bond geometry as well as tight van der Waals packing in ERG-fengycin interactions, which may be required to inhibit fengycin cluster formation and membrane permeabilization. Understanding the effect of CHOL on fengycin activity in terms of a miscibility enhancement, it is interesting to note that also the miscibility with the membrane lipids is much better for CHOL than ERG. Typical solubility limits of ERG (43-45) are in the range of 30 to 35 mol%, whereas 60 to 70 mol% have been reported for CHOL (44). Of course, the lower ability of ERG to order membranes (40) may also influence the activity of fengycin.

Impaired lipopeptide demixing and cluster formation also explain how fengycins are inhibited in the presence of anionic lipids in contrast to surfactins (Fig. 5, *B* and *C*), even though both types of lipopeptides are overall anionic. As predicted by MD simulations (20), the positively charged ornithine residue of fengycins does not dominate the overall charge of the lipopeptides, but can form favorable contacts with negatively charged PG headgroups. This, again, stabilizes the lipopeptide-lipid mixture and opposes fengycin demixing and aggregation, which are prerequisites of its membrane perturbing activity.

The high sensitivity of fengycin leakage to the negative curvature-strain lipid POPE (Fig. 6 *B*) suggests that once lipopeptide clusters are formed, their mode of action strongly relies on the formation of positive curvature strain, which has also been predicted by MD simulations (20).

Surfactin obeys default selectivity criteria

Leakage by surfactins was largely unaffected in the presence of sterols (Figs. 1 *C* and 2 *C*), was enhanced by negatively charged POPG (Fig. 5 *C*), and was slightly inhibited by the negative curvature-strain lipid POPE (Fig. 6 *C*). The effect of CHOL on surfactins resembled that of detergents (46) and differed fundamentally from that on fengycins. Namely, CHOL reduced the membrane content, R_e, of surfactins necessary to induce leakage (Table 2). Overall, these (and possibly other) effects all cancelled out to a large degree so that c_{E20} remained virtually unaffected. A reduced R_e also points to less favorable mixing and indeed, CHOL rendered the leakage mechanism from homogeneously graded, which implies a general destabilization of the membrane toward all-or-none (Fig. 3, *D* and *F*), suggesting a more local action leading to a more specific defect structure.

Two other groups reported inhibition of surfactins by CHOL based on leakage assessed through initial rates of dye release (12,14). This is less arbitrary a number than leakage after 1 h but can potentially be problematic. For

example, antimicrobial agents usually kill bacteria on timescales >1 h (47). Only in special cases it is true that leakage is monoexponential and proceeds all the way to 100%. Only then, higher initial rates imply stronger activity after biologically relevant interaction times. For detergent-like membrane permeabilizers such as surfactin, we have observed a biphasic behavior including fast but limited, graded leakage followed by slow, yet ultimately complete, pore formation (8,48). The shift to all-or-none after 1 h induced by CHOL (Fig. 3 *F*) implies that the second, slow effect becomes dominating in the presence of CHOL. General membrane destabilization and asymmetry stress, which were argued to underlie the fast graded leakage, are likely to be opposed by CHOL. It is therefore logical that CHOL reduces the initial rate of leakage but not long-term leakage and, probably, biological activity.

Negatively charged POPG enhances leakage by surfactins (Fig. 5 *C*). Because surfactins carry two acidic residues one of which is effectively charged under physiological salt and pH (33), one expects membrane binding to be opposed by anionic lipids such as POPG. However, this seems to be overcompensated by a stronger activity of membrane-bound surfactins (13). First, equilibrium head-head distances are increased by electrostatic repulsion, which enhances the positive intrinsic curvature of the molecules. Second, the energetic cost of segregating charged molecules for more localized action (pore formation) is lower in a matrix of charged molecules (where charge-charge repulsion is unavoidable anyway) than of uncharged ones.

The modest inhibition by negative curvature strain implies that membrane perturbation by surfactins depends to a lower extent on positive curvature stress formation. This finding differs from the behavior of typical detergents (49), which induce high positive curvature stress in membranes and is in line with previous NMR data (50) on surfactins obtained by our group.

The interplay between surfactin, iturin, and fengycin

Different ideas have been put forward to explain why *B. subtilis* produces not one but three families of lipopeptides. As far as selectivity is concerned, some membrane components such as PE affect surfactin and fengycin activity in a similar manner, whereas others (e.g., PG) have opposite effects on surfactin and fengycin (Table 1). One may speculate that this is how certain criteria are selected to be primarily relevant, whereas the impact of other membrane properties on lipopeptide activity is attenuated. PG, for example, boosts surfactin activity by a factor of 3 (effect on inverse MIC) but inhibits fengycin to 1/32; the overall mix of SF/IT/FE (molar ratio of SF:IT:FE is 6:57:37), does not distinguish between POPC and POPG at all.

Overall, however, it should be emphasized that there is no simple additivity of the selectivity effects. Iturin, for example, which has been found inactive in our assay but is the main component of the native lipopeptide mixture produced by *B. subtilis*, may still influence the activity of the other compounds. Concerted activity tests combining the different lipopeptide families in minimum inhibitory concentration studies with a number of pathogens have revealed a subtle, cell-selective balance between synergistic and antagonistic effects (51). Again, it will be interesting to complement this work with experiments on model membranes.

CONCLUSIONS

In vesicle leakage experiments, the native SF/IT/FE mix from *B. subtilis* QST713 is only weakly inhibited by ERG but strongly inhibited by CHOL and POPE, particularly in combination with POPG. This is in line with its observed fungicidal activity.

Considering the surfactin and fengycin families individually, the selectivity of the native mixture appears to be primarily governed by fengycins. Inhibition by CHOL, ERG, and POPG are in line with correlations seen in minimum inhibitory concentration experiments with different fungi (22). The combination of cellular data and model-membrane data clarifies whether correlations between membrane components and MICs across different cells are causal or secondary.

Inhibition of fengycins by CHOL is not because of reduced membrane uptake. On the contrary, very high amounts of fengycins incorporate into the membrane without disrupting it. We speculate that CHOL prevents fengycins from cluster formation, which is a requirement for effective membrane perturbation by this particular lipopeptide (18-20).

Surfactins are much less selective toward model-membrane composition, which is in line with their general, detergent-like action (1). Surfactins are activated by POPG, apparently compensating for the inhibitory effect of POPG on fengycins such that the SF/FE/IT mix is little affected overall. Iturins did not induce leakage in the vesicles tested.

The good ability of vesicle leakage experiments to explain the selectivity of the antimicrobial action of the lipopeptides provides another support for the assumption that these compounds act, at least primarily, by permeabilizing the target membrane.

SUPPORTING MATERIAL

Five figures are available at http://www.biophysj.org/biophysj/supplemental/S0006-3495(15)00967-4.

AUTHOR CONTRIBUTIONS

S.F. performed research. S.F. and H.H. collected funding, designed research, analyzed and interpreted data, and wrote the manuscript.

ACKNOWLEDGMENTS

We thank Martin Holzer (University of Freiburg), Jana Broecker, Helen Y. Fan (both University of Toronto), and Jon Margolis (Bayer CropScience) for fruitful discussions. We gratefully acknowledge financial support to H.H. from Bayer CropScience and the Natural Sciences and Engineering Research Council of Canada (NSERC) and to S.F. from the German Research Foundation (DFG).

REFERENCES

1. Ongena, M., and P. Jacques. 2008. Bacillus lipopeptides: versatile weapons for plant disease biocontrol. *Trends Microbiol.* 16:115–125.
2. Maget-Dana, R., and F. Peypoux. 1994. Iturins, a special class of pore-forming lipopeptides: biological and physicochemical properties. *Toxicology.* 87:151–174.
3. Vanittanakom, N., W. Loeffler, …, G. Jung. 1986. Fengycin—a novel antifungal lipopeptide antibiotic produced by *Bacillus subtilis* F-29-3. *J. Antibiot.* 39:888–901.
4. Vollenbroich, D., G. Pauli, …, J. Vater. 1997. Antimycoplasma properties and application in cell culture of surfactin, a lipopeptide antibiotic from *Bacillus subtilis*. *Appl. Environ. Microbiol.* 63:44–49.
5. Kracht, M., H. Rokos, …, J. Vater. 1999. Antiviral and hemolytic activities of surfactin isoforms and their methyl ester derivatives. *J. Antibiot.* 52:613–619.
6. Huang, X., Z. Lu, …, S. Yang. 2006. Antiviral activity of antimicrobial lipopeptide from *Bacillus subtilis* fmbj against pseudorabies virus, porcine parvovirus, newcastle disease virus and infectious bursal disease virus in vitro. *Int. J. Pept. Res. Ther.* 12:373–377.
7. Deleu, M., H. Razafindralambo, …, M. Paquot. 1999. Interfacial and emulsifying properties of lipopeptides from *Bacillus subtilis*. *Colloid Surface A.* 152:3–10.
8. Heerklotz, H., and J. Seelig. 2007. Leakage and lysis of lipid membranes induced by the lipopeptide surfactin. *Eur. Biophys. J.* 36:305–314.
9. Besson, F., M. J. Quentin, and G. Michel. 1989. Action of mycosubtilin on erythrocytes and artificial membranes. *Microbios.* 59:137–143.
10. Patel, H., C. Tscheka, …, H. Heerklotz. 2011. All-or-none membrane permeabilization by fengycin-type lipopeptides from *Bacillus subtilis* QST713. *Biochim. Biophys. Acta.* 1808:2000–2008.
11. Maget-Dana, R., and M. Ptak. 1995. Interactions of surfactin with membrane models. *Biophys. J.* 68:1937–1943.
12. Carrillo, C., J. A. Teruel, …, A. Ortiz. 2003. Molecular mechanism of membrane permeabilization by the peptide antibiotic surfactin. *Biochim. Biophys. Acta.* 1611:91–97.
13. Buchoux, S., J. Lai-Kee-Him, …, E. J. Dufourc. 2008. Surfactin-triggered small vesicle formation of negatively charged membranes: a novel membrane-lysis mechanism. *Biophys. J.* 95:3840–3849.
14. Oftedal, L., L. Myhren, …, L. Herfindal. 2012. The lipopeptide toxins anabaenolysin A and B target biological membranes in a cholesterol-dependent manner. *Biochim. Biophys. Acta.* 1818:3000–3009.
15. Nasir, M. N., A. Thawani, …, F. Besson. 2010. Interactions of the natural antimicrobial mycosubtilin with phospholipid membrane models. *Colloids Surface B.* 78:17–23.
16. Nasir, M. N., and F. Besson. 2011. Specific interactions of mycosubtilin with cholesterol-containing artificial membranes. *Langmuir.* 27: 10785–10792.
17. Aranda, F. J., J. A. Teruel, and A. Ortiz. 2005. Further aspects on the hemolytic activity of the antibiotic lipopeptide iturin A. *Biochim. Biophys. Acta.* 1713:51–56.
18. Deleu, M., M. Paquot, and T. Nylander. 2005. Fengycin interaction with lipid monolayers at the air-aqueous interface-implications for the effect of fengycin on biological membranes. *J. Colloid Interface Sci.* 283:358–365.
19. Deleu, M., M. Paquot, and T. Nylander. 2008. Effect of fengycin, a lipopeptide produced by *Bacillus subtilis*, on model biomembranes. *Biophys. J.* 94:2667–2679.
20. Horn, J. N., A. Cravens, and A. Grossfield. 2013. Interactions between fengycin and model bilayers quantified by coarse-grained molecular dynamics. *Biophys. J.* 105:1612–1623.
21. Eeman, M., G. Francius, …, M. Deleu. 2009. Effect of cholesterol and fatty acids on the molecular interactions of fengycin with stratum corneum mimicking lipid monolayers. *Langmuir.* 25:3029–3039.
22. Wise, C., J. Falardeau, …, T. J. Avis. 2014. Cellular lipid composition affects sensitivity of plant pathogens to fengycin, an antifungal compound produced by *Bacillus subtilis* strain CU12. *Phytopathology.* 104:1036–1041.
23. van Meer, G., D. R. Voelker, and G. W. Feigenson. 2008. Membrane lipids: where they are and how they behave. *Nat. Rev. Mol. Cell Biol.* 9:112–124.
24. Cerbón, J., and V. Calderón. 1991. Changes of the compositional asymmetry of phospholipids associated to the increment in the membrane surface potential. *Biochim. Biophys. Acta.* 1067:139–144.
25. Boon, J. M., and B. D. Smith. 2002. Chemical control of phospholipid distribution across bilayer membranes. *Med. Res. Rev.* 22: 251–281.
26. Epand, R. F., P. B. Savage, and R. M. Epand. 2007. Bacterial lipid composition and the antimicrobial efficacy of cationic steroid compounds (Ceragenins). *Biochim. Biophys. Acta.* 1768:2500–2509.
27. Heerklotz, H., A. D. Tsamaloukas, and S. Keller. 2009. Monitoring detergent-mediated solubilization and reconstitution of lipid membranes by isothermal titration calorimetry. *Nat. Protoc.* 4:686–697.
28. Patel, H., C. Tscheka, and H. Heerklotz. 2009. Characterizing vesicle leakage by fluorescence lifetime measurements. *Soft Matter.* 5:2849–2851.
29. Patel, H., Q. Huynh, …, H. Heerklotz. 2014. Additive and synergistic membrane permeabilization by antimicrobial (lipo)peptides and detergents. *Biophys. J.* 106:2115–2125.
30. Amaro, M., R. Šachl, …, M. Hof. 2014. Time-resolved fluorescence in lipid bilayers: selected applications and advantages over steady state. *Biophys. J.* 107:2751–2760.
31. Almeida, P. F. 2014. Membrane-active peptides: binding, translocation, and flux in lipid vesicles. *Biochim. Biophys. Acta.* 1838:2216–2227.
32. Heerklotz, H., and J. Seelig. 2001. Detergent-like action of the antibiotic peptide surfactin on lipid membranes. *Biophys. J.* 81:1547–1554.
33. Fan, H. Y., M. Nazari, …, H. Heerklotz. 2014. Utilizing zeta potential measurements to study the effective charge, membrane partitioning, and membrane permeation of the lipopeptide surfactin. *Biochim. Biophys. Acta.* 1838:2306–2312.
34. Wenk, M. R., T. Alt, …, J. Seelig. 1997. Octyl-beta-D-glucopyranoside partitioning into lipid bilayers: thermodynamics of binding and structural changes of the bilayer. *Biophys. J.* 72:1719–1731.
35. Gray, K. C., D. S. Palacios, …, M. D. Burke. 2012. Amphotericin primarily kills yeast by simply binding ergosterol. *Proc. Natl. Acad. Sci. USA.* 109:2234–2239.
36. Epand, R. M., and R. F. Epand. 2011. Bacterial membrane lipids in the action of antimicrobial agents. *J. Pept. Sci.* 17:298–305.
37. Wimley, W. C., and K. Hristova. 2011. Antimicrobial peptides: successes, challenges and unanswered questions. *J. Membr. Biol.* 239:27–34.
38. Schütte, O. M., A. Ries, …, D. B. Werz. 2014. Influence of Gb3 glycosphingolipids differing in their fatty acid chain on the phase behaviour of solid supported membranes: chemical syntheses and impact of Shiga toxin binding. *Chem. Sci. (Camb.).* 5:3104–3114.
39. Deleu, M., J. M. Crowet, …, L. Lins. 2014. Complementary biophysical tools to investigate lipid specificity in the interaction between bioactive molecules and the plasma membrane: a review. *Biochim. Biophys. Acta.* 1838:3171–3190.

40. Mannock, D. A., R. N. Lewis, …, R. N. McElhaney. 2010. The effect of variations in phospholipid and sterol structure on the nature of lipid-sterol interactions in lipid bilayer model membranes. *Chem. Phys. Lipids.* 163:403–448.

41. Scheidt, H. A., T. Meyer, …, D. Huster. 2013. Cholesterol's aliphatic side chain modulates membrane properties. *Angew. Chem. Int. Ed. Engl.* 52:12848–12851.

42. Scheidt, H. A., P. Muller, …, D. Huster. 2003. The potential of fluorescent and spin-labeled steroid analogs to mimic natural cholesterol. *J. Biol. Chem.* 278:45563–45569.

43. Mannock, D. A., R. N. Lewis, and R. N. McElhaney. 2010. A calorimetric and spectroscopic comparison of the effects of ergosterol and cholesterol on the thermotropic phase behavior and organization of dipalmitoylphosphatidylcholine bilayer membranes. *Biochim. Biophys. Acta.* 1798:376–388.

44. Stevens, M. M., A. R. Honerkamp-Smith, and S. L. Keller. 2010. Solubility limits of cholesterol, lanosterol, ergosterol, stigmasterol, and β-sitosterol in electroformed lipid vesicles. *Soft Matter.* 6:5882–5890.

45. Urbina, J. A., S. Pekerar, …, E. Oldfield. 1995. Molecular order and dynamics of phosphatidylcholine bilayer membranes in the presence of cholesterol, ergosterol and lanosterol: a comparative study using 2H-, 13C- and 31P-NMR spectroscopy. *Biochim. Biophys. Acta.* 1238:163–176.

46. Heerklotz, H. 2008. Interactions of surfactants with lipid membranes. *Q. Rev. Biophys.* 41:205–264.

47. Thoma, L. M., B. R. Boles, and K. Kuroda. 2014. Cationic methacrylate polymers as topical antimicrobial agents against Staphylococcus aureus nasal colonization. *Biomacromolecules.* 15:2933–2943.

48. Hovakeemian, S. G., R. Liu, …, H. Heerklotz. 2015. Correlating antimicrobial activity and model membrane leakage induced by nylon-3 polymers and detergents. *Soft Matter.* 11:6840–6851.

49. Madden, T. D., and P. R. Cullis. 1982. Stabilization of bilayer structure for unsaturated phosphatidylethanolamines by detergents. *Biochim. Biophys. Acta.* 684:149–153.

50. Heerklotz, H., T. Wieprecht, and J. Seelig. 2004. Membrane perturbation by the lipopeptide surfactin and detergents as studied by deuterium NMR. *J. Phys. Chem. B.* 108:4909–4915.

51. Liu, J., I. Hagberg, …, T. J. Avis. 2014. Interaction of antimicrobial cyclic lipopeptides from *Bacillus subtilis* influences their effect on spore germination and membrane permeability in fungal plant pathogens. *Fungal Biol.* 118:855–861.